

## PARTICLE ACCELERATION IN STRESSED CORONAL MAGNETIC FIELDS

R. TURKMANI,<sup>1</sup> L. VLAHOS,<sup>2</sup> K. GALSQAARD,<sup>3</sup> P. J. CARGILL,<sup>1</sup> AND H. ISLIKER<sup>2</sup>

Received 2004 July 27; accepted 2004 December 23; published 2005 January 12

### ABSTRACT

This Letter presents an analysis of particle acceleration in a model of the complex magnetic field environment in the flaring solar corona. A slender flux tube, initially in hydrodynamic equilibrium, is stressed by random photospheric motions. A three-dimensional MHD code is used to follow the stochastic development of transient current sheets. These processes generate a highly fragmented electric field, through which particles are tracked using a relativistic test particle code. It is shown that both ions and electrons are accelerated readily to relativistic energies in times of order  $10^{-2}$  s for electrons and  $10^{-1}$  s for protons forming power-law distributions in energy.

*Subject headings:* acceleration of particles — Sun: flares

### 1. INTRODUCTION

Understanding how particles are accelerated in solar flares is a major scientific challenge due to both the large number of accelerated particles ( $\sim 10^{38}$  electrons  $s^{-1}$ ) and their impulsive nature, which implies high efficiency for the acceleration mechanism(s).

Recent observations from the *Ramaty High-Energy Solar Spectroscopic Imager (RHESSI)* spacecraft have demonstrated unambiguously that between 10% and 50% of energy release in solar flares ends up in high-energy electrons. To this must be added an unknown, but probably significant, level of energization of protons and other ions (e.g., Miller et al. 1997). *RHESSI* results have also demonstrated that photon spectra have a power-law energy spectrum extending over a few decades consisting of either a single or double power law, combined in many cases with a thermal part. One conclusion is that the scaleless power-law spectra are more consistent with particle acceleration at multiple small sites rather than at a single large one (e.g., Lin et al. 2003).

The major difficulty in accounting for these observations lies in the fact that fast energy release and particle acceleration occur most effectively on small spatial and temporal scales (subkilometer and subsecond), perhaps in the vicinity of current sheets or shocks, and are best described by a full kinetic description of the plasma. On the other hand, observations indicate that a flare encompasses vast regions of the corona (many thousands of kilometers), is probably determined by the response of the coronal field to motions in the photosphere, and will be governed by a magnetohydrodynamic (MHD) description. Developing a flare model that addresses both aspects is stymied by the disparate timescales associated with the two regimes.

Many articles have addressed the problem of particle acceleration in flares from the viewpoint of a single reconnection site, shock, or a volume filled with MHD waves (see Miller et al. 1997 and Miller 1998 for a discussion). All such models are very loosely connected to the magnetic energy release process(es). It is likely that direct electric fields, MHD turbulence, and shocks are all present in the vicinity of current sheets during

magnetic reconnection, or during the initial phase of an expanding magnetic structure (coronal mass ejection), but very little is known about how these processes can energize large numbers of electrons and ions during the impulsive phase (lasting only several seconds).

It thus seems clear that understanding flare particle acceleration may require a change in our perception of the coronal magnetic topology in which energy is released. The formation of many dissipation regions that operate as acceleration sites is an interesting alternative scenario to a single monolithic site of energy release and particle acceleration (Masuda et al. 1994). In such fragmented energy release processes, particles can interact with multiple acceleration sites (e.g., Anastasiadis et al. 1997, 2004; Vlahos et al. 2004), and in principle the acceleration at one site can influence the acceleration properties of the others. Recent work along these lines has considered particle acceleration from a viewpoint that tracks “test particles” in a statistically distributed electric field resulting from many small reconnection sites using a cellular automata model (e.g., Vlahos et al. 2004; Anastasiadis et al. 2004) or fully developed MHD turbulence (Dmitruk et al. 2003; Arzner & Vlahos 2004). However, to address the acceleration problem fully, particle acceleration needs to be considered in the context of a realistic coronal magnetic field model. That is the purpose of this Letter. We use a three-dimensional MHD model to determine the coronal field structure as it responds to photospheric motions and calculate the evolution of charged particles in the electric fields generated by the stressed magnetic fields.

### 2. MODEL DESCRIPTION

The coronal field model used in this article is based on the work of Galsgaard & Nordlund (1996) and Galsgaard (2002), who performed a series of three-dimensional MHD experiments demonstrating how small-scale coronal structure (such as current sheets) arise from a sequence of simple photospheric boundary motions. The coronal field is assumed to be anchored in the photosphere at both ends, and is “straightened out:” i.e., large-scale magnetic field curvature is ignored. The initial magnetic field is uniform everywhere, while the density changes by a factor of 1000 between the photosphere and the corona. The atmosphere is initially in hydrostatic equilibrium. Photospheric motions are then imposed at the boundaries using a simple sinusoidal incompressible shear pattern that is randomly changed in time. These boundaries are impenetrable and infinitely conducting so that the imposed boundary motions advect

<sup>1</sup> Space and Atmospheric Physics Group, Imperial College, Prince Consort Road, London SW7 2BW, UK; r.turkmani@ic.ac.uk, p.cargill@ic.ac.uk.

<sup>2</sup> Department of Physics, University of Thessaloniki, 54124 Thessaloniki, Greece; vlahos@astro.auth.gr, isliker@astro.auth.gr.

<sup>3</sup> Niels Bohr Institute for Astronomy, Physics, and Geophysics, University of Copenhagen, Juliane Maries Vej 30, Copenhagen DK-2100, Denmark; kg@astro.ku.dk.

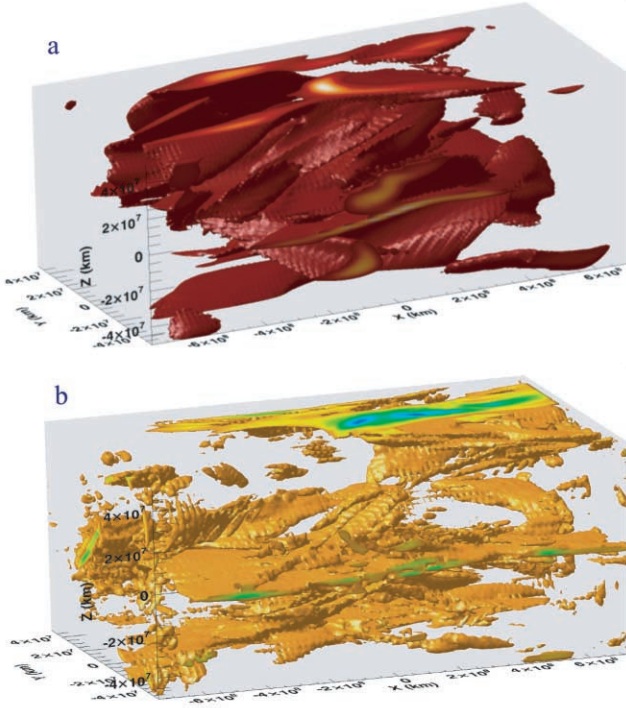


FIG. 1.—Snapshots of (a) the inductive electric field and (b) the resistive electric field configurations within the coronal volume, as calculated from the global MHD model. The details of the model are described in the text.

the magnetic footpoints with it and impose stress on the entire system.

The time-dependent evolution is followed by numerically solving the three-dimensional nonideal MHD equations in Cartesian geometry (Nordlund & Galsgaard 1997) including heat conduction and optically thin radiation. After a few driving periods, the magnetic field develops a topology that is highly structured, with strong current concentrations being scattered around the simulation box. More details about the specific numerical experiment are given in Galsgaard (2002), while a discussion of the current sheet formation and distribution is given in Galsgaard & Nordlund (1996).

To study particle acceleration, we chose a snapshot of the coronal magnetic and electric fields and ran test particles through them by solving numerically the relativistic equations of motion. The particle algorithm uses an adaptive time step and also requires values of both the magnetic and electric fields at arbitrary positions. These are determined using simple linear interpolation from the MHD solution. The electric field is fully three-dimensional and arises from two distinct sources:

$$\mathbf{E} = -\mathbf{V} \times \mathbf{B} + \eta^* \mathbf{J}, \quad (1)$$

where the first term is the inductive field and the second is the resistive field, which arises as a result of a finite resistivity, and  $\mathbf{V}$  is the plasma velocity given by the MHD equations. The MHD code utilizes a hyperresistivity  $\eta^*$  to localize diffusion only to regions where it is required in order to limit steepening of nonlinearities (for details, see Nordlund & Galsgaard 1997). Figures 1a and 1b show a snapshot of the coronal resistive and inductive fields, respectively, for a simulation with dimensions  $2 \times 10^8$  cm in the transverse ( $y$  and  $z$ ) directions and  $1.5 \times 10^9$  cm along the loop axis ( $x$ -direction). The highly fragmented structure of both field components is clear, and these are as-

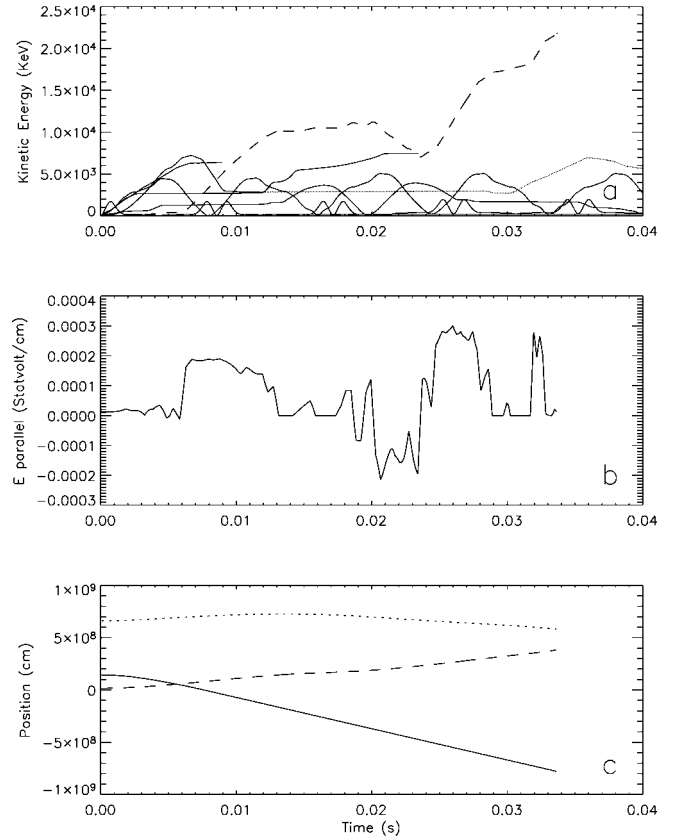


FIG. 2.—(a) Energy gain vs. time for a randomly chosen sample of 10 electrons. (b) Parallel electric field experienced by one electron, shown in panel a as a dashed curve. (c) Position of the particle given by the  $x$ -,  $y$ -, and  $z$ -positions denoted as solid, dotted, and dashed curves, respectively. The  $y$ - and  $z$ -positions are multiplied by a factor of 10.

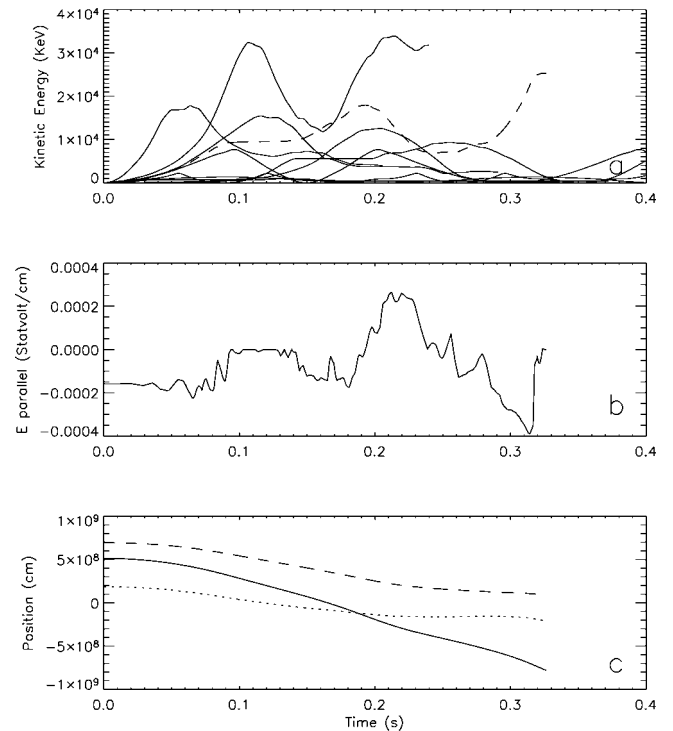


FIG. 3.—Same as Fig. 2, but for a randomly chosen sample of 10 protons.

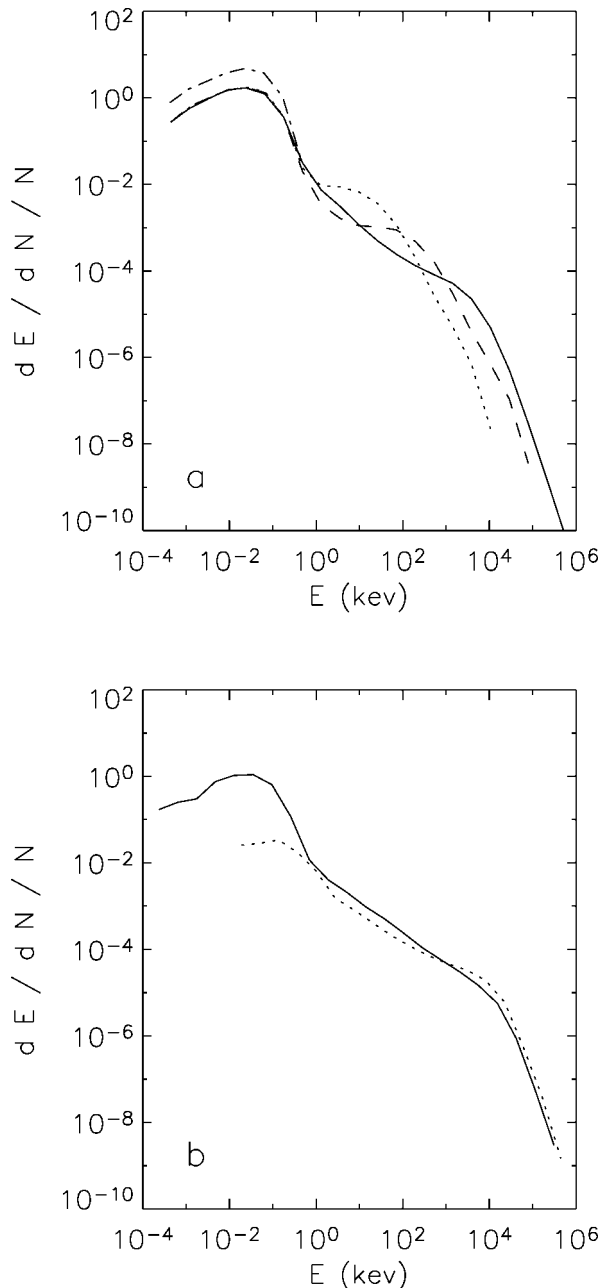


FIG. 4.—Distribution function obtained by running 40,000 electrons in a coronal volume with  $L = 1.5 \times 10^9$  cm. (a) The time evolution of the distribution functions taken at  $t = 0$  (dot-dashed curve; the curve terminates at  $E \sim 1$  keV),  $t_1 = 0.0125$  s (dotted curve),  $t_2 = 0.025$  s (dashed curve), and  $t_3 = 0.05$  s (solid curve). (b) The final distribution function at  $t = 0.1$  from the above model when we consider only the resistive component of the electric field (solid curve) compared to that of a similar model that considers both the resistive and the inductive components on the electric field (dotted curve).

sociated with magnetic field turbulence with a magnitude of 5%–10% of the ambient field.

One would expect the first term in equation (1) to be important outside current sheets, where it will lead to predominantly (but not solely)  $\mathbf{E} \times \mathbf{B}$  drifts, and the second in the vicinity of reconnection sites, where it will lead to acceleration parallel to the ambient magnetic field (see also Dmitruk et al. 2003). We focus predominately on cases using the resistive field only, since that is where one expects the predominant energy gain to come from. However, we compare these results to models including both electric field components.

We adopt the following initial physical parameters for the MHD model. The coronal  $\beta$  is small, and the magnetic field is taken as 100 G in the axial ( $x$ ) direction. The anomalous resistivity  $\eta^*$  is either zero or takes on values between  $10^{-1}$  and  $10^{-3}$  s. These parameters then determine the strength and orientation of the electric field from Maxwell's equations and Ohm's law. We use only the coronal part of the MHD model. Particles that leave the coronal region are considered lost from our system. Both electrons and protons are tracked. We inject the particles starting from a Maxwellian distribution with a temperature of  $\sim 1.2 \times 10^6$  K (Fig. 4a, dot-dashed curve). The initial positions of the particles are random, as is their pitch angle.

### 3. RESULTS

Figure 2 shows the properties of 10 arbitrarily chosen electrons. Figure 2a shows the energy of the particles versus time, Figure 2b shows the parallel electric field experienced by the particle shown as a dashed curve in panel a, and Figure 2c shows the position of this particle. Figure 3 shows the same parameters as Figure 2 but for 10 arbitrarily chosen protons. Some of the particles gain a little energy, some gain and then lose energy, while a few reach high energies. The timescale for energy gain is significantly less than 1 s for electrons that get accelerated to tens of MeV within a few times  $10^{-2}$  s. Protons reach roughly the same energy within a few times  $10^{-1}$  s, and both timescales are much shorter than any MHD timescale.

As they undergo acceleration, the particles move through a large portion of the simulation box and so experience acceleration at a number of current sheets. Some particles exit the box quickly, while others remain trapped inside for a longer time. Because of the nature of the photospheric driver, the axial current (and hence  $E_{\parallel}$ ) can take on either positive or negative values, depending on the nature of the shear in the coronal field. As the particles interact with a current sheet, the reconnection of the field there means that they can move through the simulation, hence sampling flux systems with different photospheric connectivity. Note also that the parallel electric field is 2–3 orders of magnitude in excess of the Dreicer field.

Particles tend to travel along the field lines if the inductive field is not included. If it is included, the electrons stay close to the field lines while protons tend to travel initially away from the field lines and then bend and join the trajectory of a field line. This is similar to the familiar “ion pickup” phenomenon. This is due to the fact that for a proton and an electron with the same initial energy, electrons have a higher velocity, which makes contribution from the drift velocity negligible compared to their initial one.

Figure 4a shows the time evolution of the distribution functions obtained from running 40,000 electrons inside a box for a time long enough to allow all free particles to leave the box (0.1 s). The dot-dashed curve shows the initial distribution at  $t = 0$ , whereas the dotted, dashed, and solid curves show the distribution function at  $t_1 = 0.0125$  s,  $t_2 = 0.025$  s, and  $t_3 = 0.05$  s, respectively. The final distribution function is shown as the solid curve in Figure 4b and is obtained by considering all the particles, including those that left the box before the end of the run. Figure 4a shows that while a certain population of the particles maintain their initial Maxwellian distribution below 1 keV, a tail develops gradually toward the MeV region ending with a cutoff at high energies. In Figure 4b, the final distribution function shows a pronounced

power-law component between 1 keV and 10 MeV, whereas the distribution after the cutoff extends toward 0.5 GeV.

The dotted curve in Figure 4*b* shows the distribution function resulting from a run that uses both the resistive and inductive electric field components. It shows that the inductive field plays a very small role in the overall acceleration. This is mainly because the parallel component of this field must be zero, and the energy gain in the perpendicular direction is very small compared to that from the parallel resistive field component. However, this perpendicular contribution does show an effect in the region below 1 keV. Particles that remain within this range are mainly those injected in regions where the parallel resistive field is zero. They therefore maintain their thermal distribution but gain some energy when the inductive field is included.

We have examined the scaling of the results with the length of the box. The maximum energy scales up with the length of the domain. A temporal scaling also arises here as particles need more time to travel through a longer domain.

#### 4. DISCUSSION AND CONCLUSIONS

In this Letter, we study for the first time the acceleration of electrons and ions inside a coronal magnetic flux tube stressed by the random motions of the photosphere using a three-

dimensional MHD code. The stochastic development of current sheets that are associated with a distribution of strong electric fields inside the stressed magnetic topology provide the electromagnetic environment in which particles are accelerated. Using a relativistic test particle code, we follow the evolution of an ensemble of electrons and ions. Our main finding is that the electrons and ions are accelerated fast and efficiently along the entire length of the magnetic structure. In relatively short times, particles reach relativistic energies and form power-law distributions in energy. We also found that the inductive electric field plays a very small role in accelerating particles.

We conclude that the stochastic formation of current sheets in magnetic topologies that are complex and stressed by the photosphere can provide an alternative to the existing models for solar flares.

This work was funded by the European Commission under research training network HPRN-CT-2001-00310. K. G. acknowledges funding by PPARC in the form of an Advanced Fellowship and Carlsbergfondet in the form of a scholarship over various periods of the project. P. J. C. acknowledges the support of a PPARC senior fellowship. The numerical MHD experiments were carried out on the UK Astrophysical Fluids Facility.

#### REFERENCES

- Anastasiadis, A., Gontikakis, C., Vilmer, N., & Vlahos, L. 2004, *A&A*, 422, 323
- Anastasiadis, A., Vlahos, L., & Georgoulis, M. K. 1997, *ApJ*, 489, 367
- Arzner, K., & Vlahos, L. 2004, *ApJ*, 605, L69
- Dmitruk, P., Matthaeus, W. H., Seenu, N., & Brown, M. R. 2003, *ApJ*, 597, L81
- Galsgaard, K. 2002, in *IAU Colloq. 188, SOLMAG 2002*, ed. H. Sawaya-Lacoste (ESA SP-505; Noordwijk: ESA), 269
- Galsgaard, K., & Nordlund, Å. 1996, *J. Geophys. Res.*, 101, 13445
- Lin, R. P., et al. 2003, *ApJ*, 595, L69
- Masuda, S., Kosugi, T., Hara, H., Tsuneta, S., & Ogawara, Y. 1994, *Nature*, 371, 495
- Miller, J. A. 1998, *Space Sci. Rev.*, 86, 79
- Miller, J. A., et al. 1997, *J. Geophys. Res.*, 102, 14631
- Nordlund, Å., & Galsgaard, K. 1997, *A Three-Dimensional MHD Code for Parallel Computers* (Tech. Rep.; Copenhagen: Astron. Obs., Copenhagen Univ.)
- Vlahos, L., Isliker, H., & Lepreti, F. 2004, *ApJ*, 608, 540